

AN EMPIRICAL MODEL OF THE EARTH'S PLASMASPHERE

D. L. Gallagher,* P. D. Craven* and R. H. Comfort**

* NASA Marshall Space Flight Center, Huntsville, AL 35812, U.S.A.

** University of Alabama in Huntsville, Huntsville, AL 35899, U.S.A.

ABSTRACT

We present here an empirical model of plasmaspheric low energy plasma consisting of H⁺. The model is developed from a data base derived from measurements taken by the Retarding Ion Mass Spectrometer on the Dynamics Explorer 1 satellite. An analytical expression that reproduces the density profiles for moderate geomagnetic activity is given and discussed. This expression reproduces the density fall off in the ionosphere as well as the sharp density decrease at the plasmapause.

INTRODUCTION

Although the plasmasphere and magnetosphere have been the object of study for several years, no comprehensive empirical model exists for these regions of space. Empirical models do exist for more limited spatial regions. Figure 1 shows schematically the regions of space covered by these models. The models of Garrett and DeForest /1/ for geosynchronous orbit, Brace and Theis /2/ and Kohlein /3/ for electron and ion temperatures in the ionosphere, and Persoon et al. /4/ for the polar cap are examples of such models. An accurate empirical model of the plasmasphere and inner magnetosphere is needed for comparison with theoretical models and in studies of other planetary bodies. Numerical models do exist for some of these regions, e.g. the numerical model for the plasmasphere described by Young et al. /5/. The advantage of empirical models is that they can give good quantitative results with only modest requirements on computer time and memory.

The empirical model presented here follows a slightly different approach than that given by Gallagher and Craven /6/, in that, measurements of plasmaspheric density profile are grouped before being fit by an analytical expression. In addition, a more comprehensive analytical function is used as the base or zero-order fit. In the previous study, corrections were required (in the form of Gaussian functions) to the zero-order function in order to reproduce measured plasmaspheric density. The present function is applicable over a wider range of altitudes, extending from the bottom side ionosphere to just beyond the plasmapause, as will be discussed below. An apparent advantage of the new analytical function over the previous function given by Gallagher and Craven /6/ is that Gaussian corrections may not be required.

Due to the dynamic character of the plasmasphere, care must be taken in the statistical treatment of plasmaspheric measurements. Averages over measurements from different times or different geophysical conditions may result in the distortion of plasmaspheric features. This study attempts to minimize statistical smoothing by grouping together measurements that present similar profiles of plasmaspheric density before seeking an analytical representation of the data. In addition, the current modeling effort is intended only to reproduce large scale features of the plasmasphere and plasmapause. Small scale and dynamic features, such as multiple plasmapause boundaries and detached plasma regions, are not yet included in the model.

Currently reduced RIMS measurements constitute a sufficient base of information to adequately represent the plasmasphere from 0000 hours to 1200 hours magnetic local time and between $\pm 40^\circ$ magnetic latitude. RIMS measurements in regions other than these have been reduced but are not yet as numerous. The range of spatial coverage possible in four different local time sectors from the Dynamics Explorer 1 satellite is given by Gallagher and Craven /6/ (their Figure 1). The spatial coverage available for this report and for the same four local time sectors as used by Gallagher and Craven is shown in Figure 2. Each of the four panels represents a meridional, half-plane cross section of the locations of available RIMS measurements in a 6-hour interval of magnetic local time. As the processing of RIMS

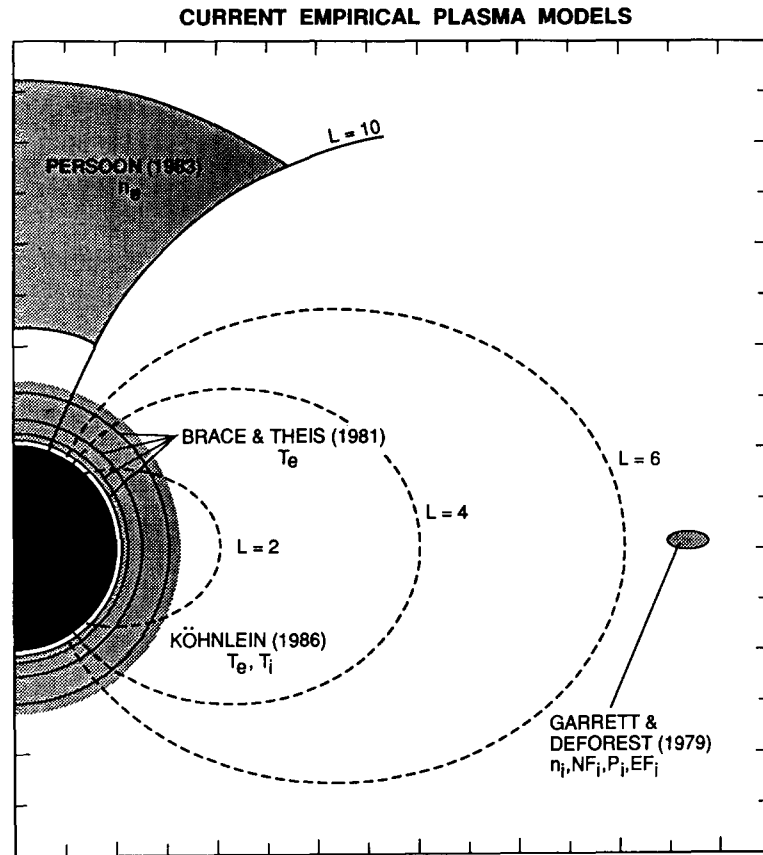


Fig. 1. The regions described by currently available empirical models of the near Earth magnetosphere are sketched. Included in these models are descriptions of ion temperatures below 4000 km altitude, ion fluxes and densities at geosynchronous altitudes, and electron densities in the polar cap.

measurements continues, the available information for this empirical modeling effort will eventually approximate that of the total possible spatial coverage.

DATA ANALYSIS

The analysis of DE 1 RIMS observations (for instrument description see /7/) is accomplished by the use of computer automated software that determines density, temperature and flow velocity independently for each of the ion species measured. Although the ion species measured by RIMS are programmable and have varied somewhat since the early part of the mission, measurements of the major ion species, H⁺, He⁺, and O⁺, are almost always available. The analysis makes use of the thin-sheath approximation /8,9/ to determine the densities and temperatures of the ions. The thin sheath approximation takes into account the effects of spacecraft potential on the observation of very low energy ion populations.

Care is taken to exclude ion measurements that cannot yet be interpreted by automated processing. Very low densities and/or high positive spacecraft potentials can result in very low count rates. When the counts per sampling period fall below 10, these measurements are excluded from the study. Measurements are also excluded when they are very noisy or show evidence of non-isotropic distributions, e.g. field-aligned, conic, or trapped ion distributions.

The RIMS instrument consists of one detector in the spacecraft spin plane and two along the spin axis. Particle counts versus spin phase angle are obtained from the radial RIMS detector. Normally the peak count rate from the radial detector is found to be in the direction of the spacecraft velocity vector, indicative of isotropic ion distributions. When the flux peak occurs at more than 20° from the spacecraft velocity vector, the observation is excluded from this study. These events usually occur outside the plasmasphere and are characteristic of directed plasma flows or of non-isotropic distributions which are not acceptable for the analysis techniques used in this study.

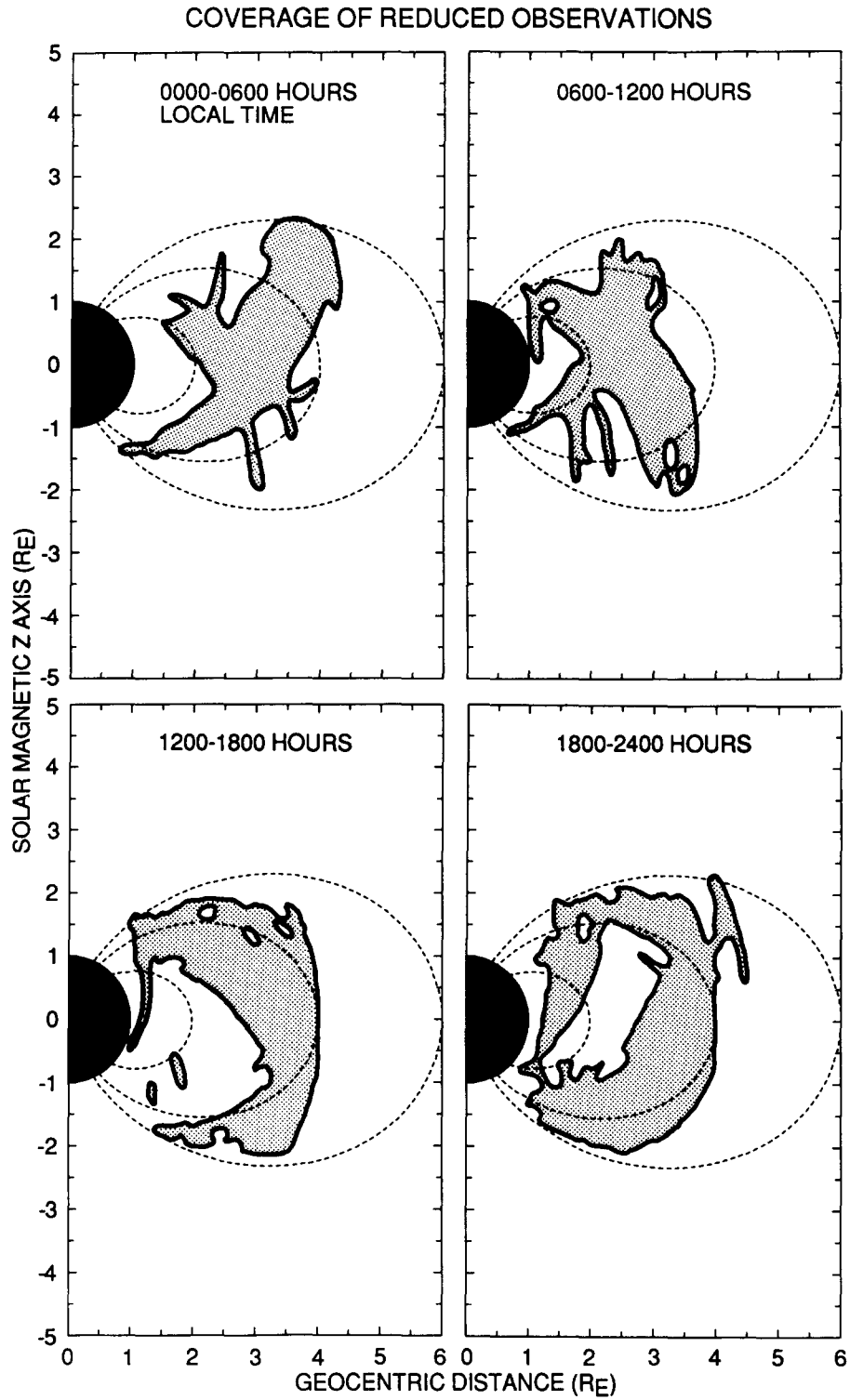


Fig. 2. The available orbital coverage of the Dynamics Explorer 1 spacecraft from 1981 through 1986 is shown in four magnetic local time intervals. The shaded areas indicate locations represented by currently reduced RIMS measurements. The earth's origin is located in the center left of each panel with $\pm 5 R_E$ along the vertical axis and $0-5 R_E$ along the horizontal axis in a meridian projection including the z-axis in solar magnetic coordinates.

Although some outer plasmaspheric measurements are lost as a consequence of these limitations and those above, more often, the measurements extend to include the plasmapause. The consequence of the limitations is that the study is essentially restricted to the plasmasphere and the plasmapause regions.

RIMS measurements do not extend beyond the plasmasphere to geosynchronous orbit and are not sufficient to characterize the ionosphere. However, it is important to insure that the plasmaspheric empirical model under development does not become unrealistic in these regions; therefore, boundary conditions are imposed at low and high altitudes. For the present, a typical daytime ionospheric profile for hydrogen from Hanson and Carlson /10/ is used. In the future, a more representative description of the ionosphere, e.g. the empirical model International Reference Ionosphere /11/ or a physical model like that described by Young *et al.* /5/ will be used. Densities at geosynchronous altitude are obtained from Higel and Lei /12/.

The results presented in this paper are from measurements during 1981 and 1982, shortly after the last solar maximum. The reduction of RIMS measurements is continuing and will extend beyond solar maximum, toward solar minimum. The continued reduction of RIMS observations is expected to provide better evidence for seasonal effects and for plasmaspheric response to a broad spectrum of geomagnetic conditions.

EMPIRICAL MODEL

Our empirical model consists of an analytical expression that can be used to reproduce hydrogen density at arbitrary locations in the plasmasphere for given conditions. The principal spatial dependence of plasmaspheric H⁺ density is on L-shell. Equations (1) - (4) give the dependence on L-shell that is currently used in this modeling effort:

$$\text{LOG}_{10}(n) = a_1 \cdot F(L) \cdot G(L) \cdot H(L), \quad (1)$$

where

$$F(L) = a_2 - e^{a_3(1 - a_4 e^{-h(L,\lambda)/a_5})}, \quad (2)$$

$$G(L) = a_6 L + a_7, \text{ and} \quad (3)$$

$$H(L) = \left(1 + \left(\frac{L}{a_8}\right)^2(a_9 - 1)\right)^{-\left(\frac{a_9}{a_9 - 1}\right)}. \quad (4)$$

The constants a_i ($i=1-9$) are free parameters used to fit equation (1) to the logarithm of ion density. L is the McIlwain L-shell parameter, $h(L,\lambda)$ is the height above the Earth's surface, and λ is geomagnetic latitude. Equation (2) is a modified Chapman layer /13/ where the $-z/H$ term has been removed from the exponential of the usual expression to prevent $F(L)$ from falling at large L-shells. Equation (3) is simply linear in L-shell and, as will be shown later, has been found to best represent inner plasmaspheric density profiles. Equation (4) has the form of a modified Lorentzian and serves to represent the location and shape of the plasmapause. When taken together in equation (1), these expressions have been found to reproduce the fundamental features of the steady state plasmasphere.

Figure 3 shows a fit of equation (1) to RIMS measurements between 8 and 12 hours magnetic local time, 15° and 30° magnetic latitude, and for a weighted Kp ranging from 2.5 to 4.5. As discussed above, the ionospheric and geosynchronous densities are obtained independently. This is a typical profile for the data grouped according to local time, magnetic latitude, and weighted Kp. Weighted Kp is an average Kp taken over the previous 5 days, where each 3-hour Kp value receives an exponential weighting factor with a 36 hour (1/e) time constant. The use of this weighted Kp is discussed below.

Like Figure 3, Figure 4 displays density versus L-shell for RIMS measurements between 15° and 30° magnetic latitude and between weighted Kp values ranging from 2.5 to 4.5. Unlike Figure 3, measurements from all local times are superimposed in the same display. The various regions outlined in Figure 4 represent density measurements in 4 hour magnetic local time intervals, centered at the times indicated. The resulting assemblage reveals an essentially linear variation of the logarithm of density with L-shell from $L=1.5$ to $L=4.5$, but where the plasmapause location and slope vary with magnetic local time. This inner plasmaspheric density variation has been found to be characteristic of all plasmaspheric density profiles so far examined. The linear variation of the logarithm of density with L-shell is reflected in equation (3) above.

Between $L=1.5$ and $L=3$, equation (1) reduces to the form

$$n(L) \propto 10^{-A \cdot L}, \quad (5)$$

where $A = a_2 \cdot a_6$.

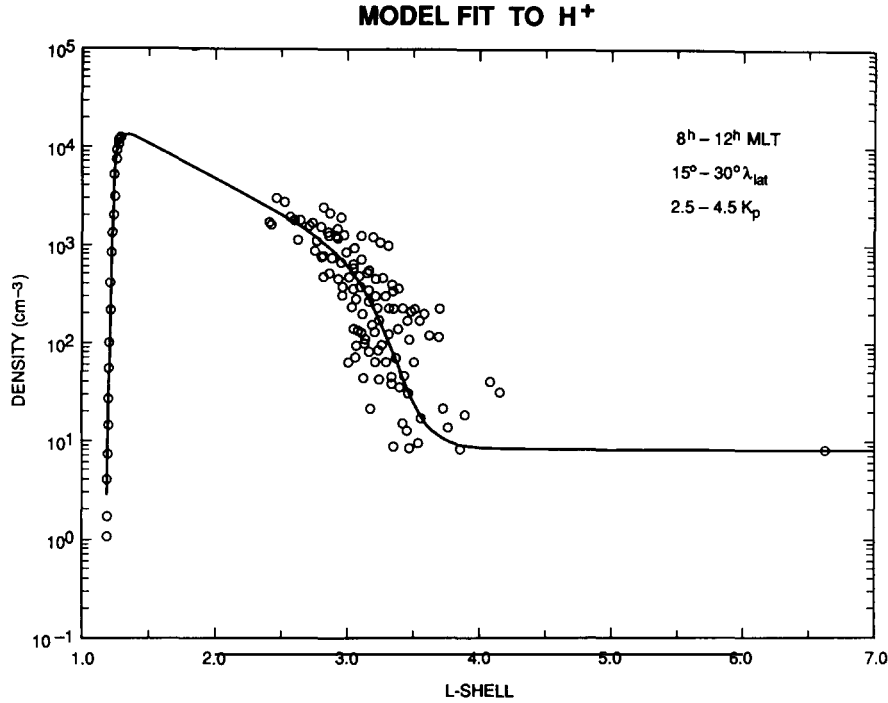


Fig. 3. The analytical expression (equation (1)) used in this empirical model is shown fit to DE 1 RIMS observations. Also shown are results for geosynchronous, equatorial ion density from Higel and Lei /12/ and ionospheric values for a modified, classic Chapman layer. RIMS measurements are between 8 hours and 12 hours magnetic local time, 15° and 30° magnetic latitude, and for weighted Kp values ranging from 2.5 to 4.5.

The procedure for producing this empirical model is to fit equation (1) to statistical profiles of density versus L-shell for various local times and latitudes and then to find analytical representations for the variation in the fit parameters a_i as a function of magnetic local time, latitude, and weighted Kp. Figure 5 shows an example of the variation of a_6 , from equation (3) above, with magnetic local time. Although the existing local time coverage is limited, an approximate fit can be found and is shown by the solid line. This fit, where x is defined in Figure 5, is given by

$$a_6 = -0.87 + 0.12e^{-x^2/3^2}. \quad (6)$$

Similar fits for a_8 and a_9 , both from equation (4) above, have been found:

$$a_8 = 0.7 \cos(2\pi \frac{MLT - 21}{24}) + 4.4 \quad (7)$$

and

$$a_9 = 15.3 \cos(2\pi \frac{MLT}{24}) + 19.7. \quad (8)$$

The parameter a_6 controls the density gradient in the inner plasmasphere, while a_8 and a_9 determine the location and slope of the plasmopause, respectively. For the density data used in this study, the other fit parameters of equation (1) are constant and given by $a_1 = 1.4$, $a_2 = 1.53$, $a_3 = -0.036$, $a_4 = 30.76$, $a_5 = 159.9$, and $a_7 = 6.27$.

The resulting picture of plasmaspheric H⁺ density is shown in Plate 1. Here, density from 15° to 45° magnetic latitude, as a function of L-shell and magnetic local time, is projected onto the solar magnetic equatorial plane. Height above the plane represents the logarithm of hydrogen density. Colored lines are used to indicate dipolar L-shells. The viewer is looking sunward from a position 30° post-midnight and 30° north of the magnetic equatorial plane. The plasmasphere is found to be nearly symmetric in local time for L < 3, with only a slight difference in the noon-midnight density gradient for these inner L-shells. Beyond an L=3, there is a clear enlargement of the plasmasphere in the evening, extending out to almost L=5 compared to a dawn plasmopause near L=4.

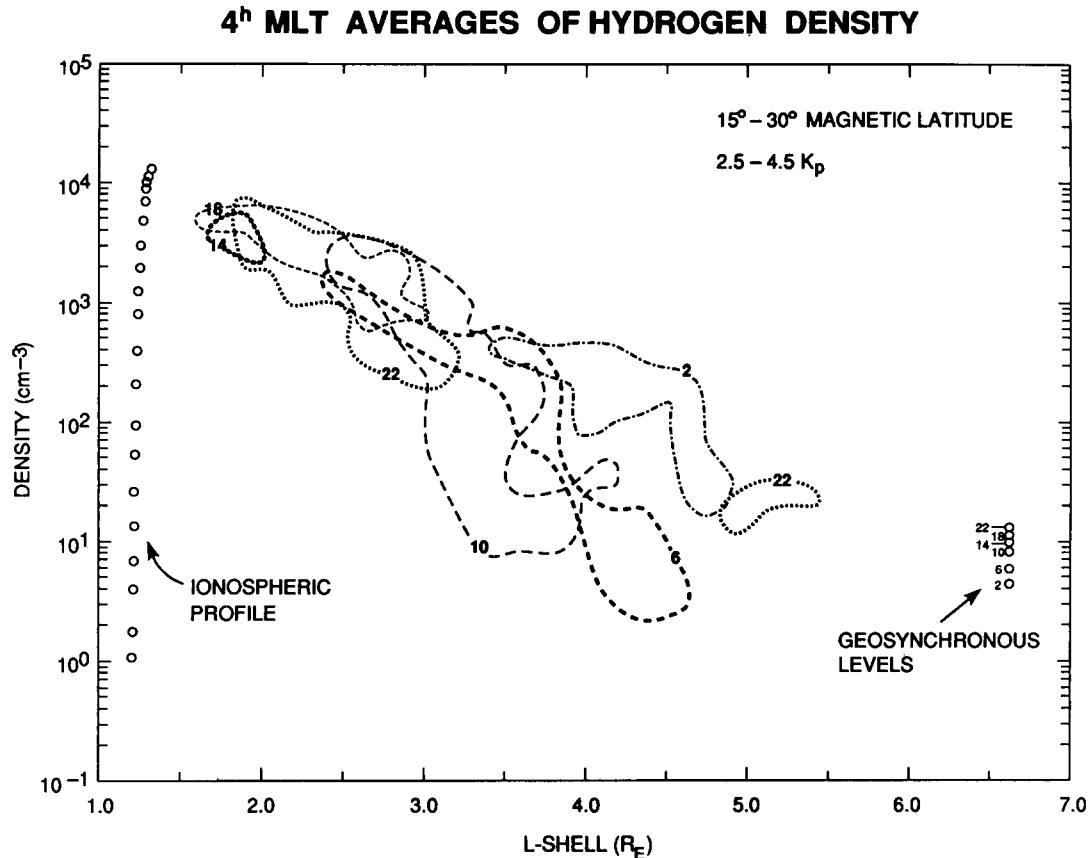


Fig. 4. Density versus L-shell is displayed for RIMS measurements between 15° and 30° magnetic latitude and between weighted K_p values ranging from 2.5 to 4.5. Measurements from all local times are superimposed in the same display. The various regions outlined in Figure 4 represent density measurements in 4 hour magnetic local time intervals, centered at the times indicated.

DISCUSSION

A leading concern in the statistical treatment of the plasmasphere is in the handling of its dynamic characteristics. Simple spatial averaging of plasmaspheric density would result in a smearing of the plasmopause and other plasmaspheric density gradients. However, some kind of collective utilization of multiple plasmaspheric measurements is required in order to obtain a realistic overall description of the plasmasphere. Our approach centers around the need to first identify a mechanism by which plasmaspheric profiles can be ordered by similarities in the condition of the plasmasphere. Once ordered, measurements of density or temperature can be averaged to develop pictures of the plasmasphere under various conditions.

Initially, displays of density versus L-shell for individual DE 1 orbit passes have been obtained. These plasmaspheric profiles were grouped by the shape of the plasmasphere at various local times and latitudes. As is expected, a range of plasmopause locations were found in each angular bin, roughly related to the level of geophysical activity, as indicated by K_p. However, the nearest 3-hour K_p average, alone, was not found to systematically group like plasmaspheric profiles. Instead, we found it necessary to incorporate K_p history. The best result in ordering plasmaspheric density profiles has been obtained by using a weighted K_p average. An average over the previous 5 days of 3-hour K_p values is obtained for each DE RIMS density measurement. Individual 3-hour K_p values are weighted by an exponential factor, which decreases backwards in time with a 1/e time constant of 3-days. The effect is to include recent K_p history, but with diminishing influence for the more distant in time.

The weighted K_p used in this study has been obtained entirely on empirical grounds. As with any selection criteria, there are cases that do not fit the mold. So far, the number of exceptions are few enough that the results are not adversely affected. We will continue to evaluate the influence of grouping plasmaspheric density measurements by weighted K_p in order to insure that overall plasmaspheric characteristics are not compromised by statistical averaging.

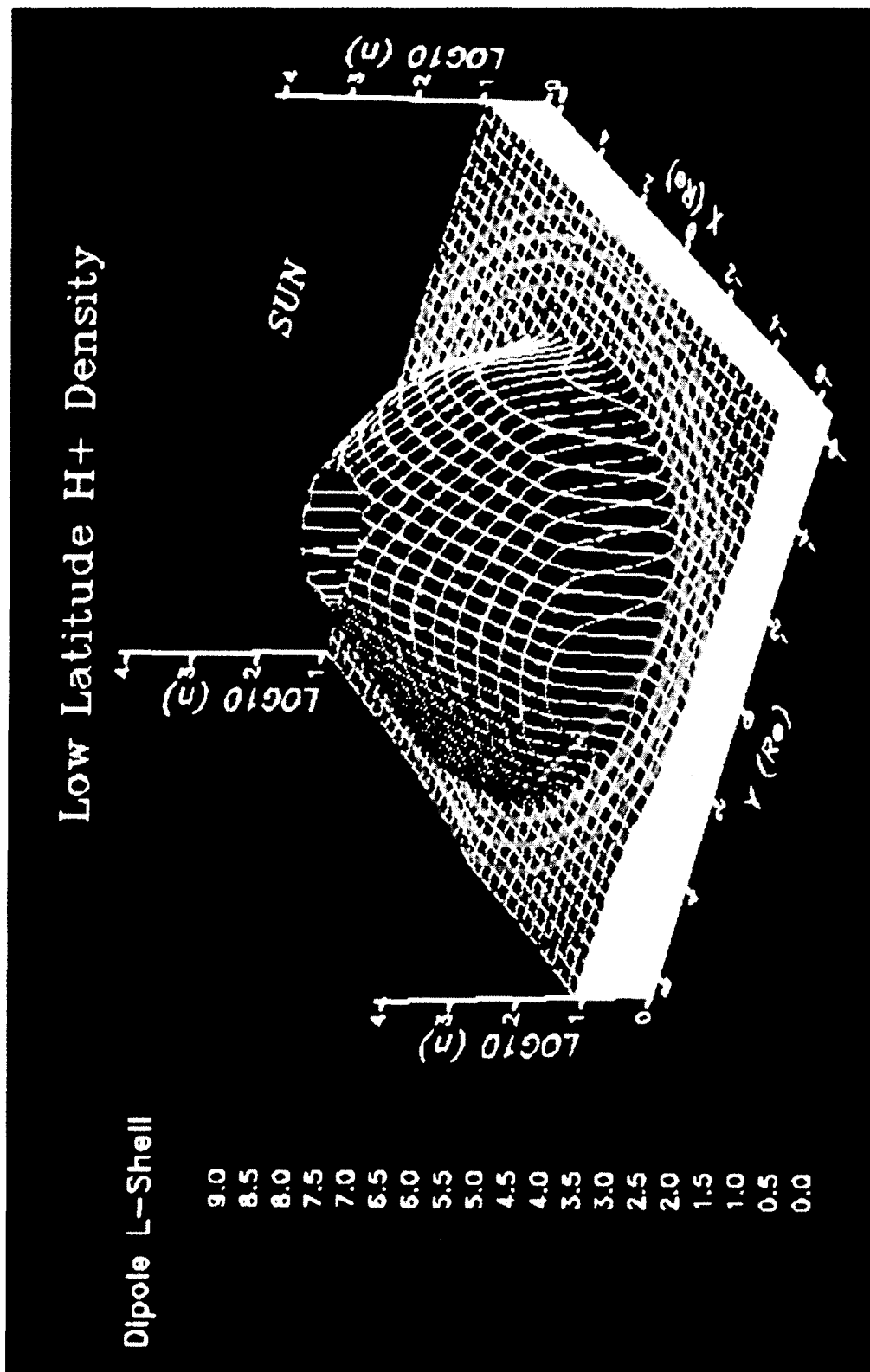


Plate 1. The resulting empirical model of plasmaspheric hydrogen density is shown. Here, density from 15°–45° magnetic latitude, as a function of L-shell and magnetic local time, is projected onto the solar magnetic equatorial plane. Height above the plane represents the logarithm of hydrogen density. Colored lines are used to indicate dipolar L-shells. The viewer's perspective is looking generally toward the Sun from a position 30° post-midnight and 30° north of the magnetic equatorial plane.

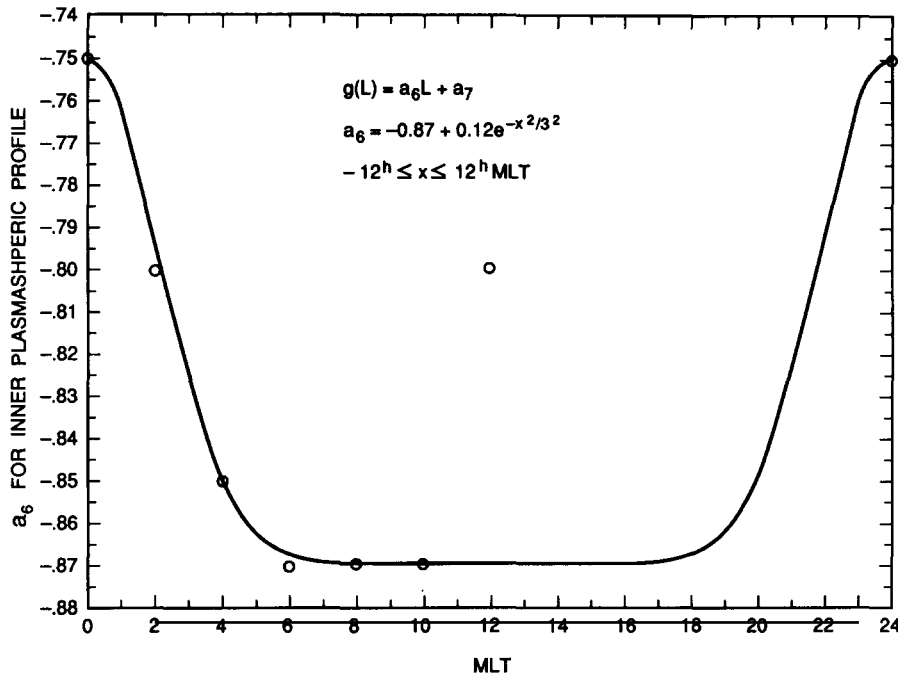


Fig. 5. This figure shows an example of the variation of a_6 , from equation (3), with magnetic local time. Although the existing local time coverage is limited, an approximate fit can be found and is shown by the solid line. Each value of a_6 results from fitting equation (1) to RIMS measurements obtained in 2-hour magnetic local time intervals, between 15° and 45° magnetic latitude, and for weighted K_p ranging from 2.5 to 4.5. The fit parameter a_6 reflects the gradient of hydrogen density in the inner plasmasphere, as shown in equations (1) and (3).

Although our modeling effort is not yet complete, two interesting plasmaspheric characteristics are emerging: the linear decrease in the logarithm of hydrogen density in the inner plasmasphere and the absence of a pronounced asymmetric density bulge in the evening plasmasphere. As noted above, previous studies have most often used a power-law variation of plasmaspheric density with L-shell. This dependence is derived from a straight forward calculation of the volume of a flux tube in terms of L-shell and the assumption that the rate of ionospheric outflow into the plasmasphere is independent of invariant latitude. The result is an anticipated $1/L^4$ variation.

Statistical measurements of density in the inner plasmasphere by RIMS currently indicate a linear variation of the logarithm of density with L-shell. The scale factor "A" from equation (5) for L-shell density dependence ranges from about -1.6 to -1.9. It is too early to conclude whether plasmaspheric density varies as a power law or like that shown in equation (5). However, the existing RIMS observations of plasmaspheric density support the behavior indicated in equation (5).

The current empirical model displays approximate azimuthal symmetry for hydrogen density inside $L=3$ and extension of the plasmasphere out to larger radial distances at evening local times. Brice /14/ and Chappell et al. /15/ also indicate symmetry at lower distances and a pronounced bulge at larger distances at dusk; although their observations are for the magnetic equator and ours are for magnetic latitudes between 15° and 45° . Our model's extension of the plasmasphere to larger radial distances at evening local times, however, does not appear to be the result of a tear-drop shaped outer plasmasphere. Our enhanced evening densities appear to be the result of an otherwise symmetric plasmaspheric density profile, which has been shifted off center toward 21 hours magnetic local time.

Although still incomplete, a new empirical model of the plasmasphere has begun to take shape. The preliminary results offer the expectation for a global multi-ion description of overall plasmaspheric characteristics. As the model is completed, it will serve as the empirical basis for extensions of both theory and empirical modeling to include the more dynamic characteristics of the plasmasphere. In addition, other sources of plasmaspheric observation may be included with the DE 1 RIMS empirical model to further extend its empirical foundation.

ACKNOWLEDGEMENTS

The authors are greatfull to D. A. Gurnett for the important use of plasma wave derived electron densities in the analysis of RIMS measurements, obtained from the University of Iowa Plasma Wave Instrument on the Dynamics Explorer 1 spacecraft. A rather large programming effort has been and continues to be required for this study. Most, if not all, of the programming has fallen on the capable shoulders of Richard West of Boeing Computer Support Services. The authors would like to acknowledge his untiring efforts and capable work. We also would like to thank those others who have contributed to the development of the empirical model especially Don Cooley, Tom Six, and Barbara Giles. The authors acknowledge the significance of using the Space Physics Analysis Network (SPAN) in this research. This research was supported by the Office of Space Science and Applications at the National Aeronautics and Space Administration. One of the authors (R.H.C.) has received support from NASA Grant NAS8-058 with the University of Alabama in Huntsville.

REFERENCES

1. H.B. Garrett and S.D. DeForest, An analytical simulation of the geosynchronous plasma environment, Planet. Space Sci. 27, 1101 (1979).
2. L.H. Brace and R.F. Theis, Global empirical models of ionospheric electron temperature in the upper F-region and plasmasphere based on in situ measurements from the Atmosphere Explorer-C, ISIS-1, and ISIS-2 satellites, Journal of Atmospheric and Terrestrial Physics 43, 1317 (1981).
3. W. Kohnlein, A model of the electron and ion temperatures in the ionosphere, Planet. Space Sci. 34, 609 (1986).
4. A.M. Persoon, D.A. Gurnett, and S.D. Shawan, Polar Cap Densities from DE 1 Plasma Wave Observations, J. Geophys. Res. 88, 10,123 (1983).
5. E.R. Young, D.G. Torr, P. Richards, and A.F. Nagy, A Computer Simulation of the Mid-latitude Plasmasphere and Ionosphere, Planet. Space Sci. 28, 881 (1980).
6. D.L. Gallagher and P.D. Craven, Initial Development of a New Empirical Model of the Earth's Inner Magnetosphere for Density, Temperature and Composition, in Modeling Magnetospheric Plasma (ed.'s T.E. Moore and J.H. Waite, Jr.), AGU Geophysical Monograph Series Vol. 44, p61, 1988.
7. C.R. Chappell, S.A. Fields, C.R. Baugher, J.H. Hoffmann, W.B. Hanson, W.W. Wright, H.D. Hammack, G.R. Carignan, and A.F. Nagy, The Retarding ion mass spectrometer on Dynamics Explorer-A, Space Sci. Instrum. 5, 477 (1981).
8. R.H. Comfort, C.R. Baugher, and C.R. Chappell, Use of the thin sheath approximation for obtaining ion temperatures from the ISEE 1 limited aperture RPA, J. Geophys. Res. 87, 5109 (1982).
9. R.H. Comfort, J.H. Waite, Jr., and C.R. Chappell, Thermal ion temperatures from the Retarding Ion Mass Spectrometer on DE 1, J. Geophys. Res. 90, 3475 (1985).
10. W.B. Hanson and H.C. Carlson, The Upper Atmosphere and Magnetosphere, Chapter 5 in The Ionosphere, National Academy of Sciences, Washington, D.C., 1977.
11. D. Bilitza, International Reference Ionosphere: Recent developments, Radio Science 21, 343 (1986).
12. B. Higel and W. Lei, Electron Density and Plasmopause Characteristics at 6.6 Re: A Statistical Study of the GEOS 2 Relaxation Sounder Data, J. Geophys. Res. 89, 1583 (1984).
13. O.K. Garriott and H. Risbeth, Introduction to Ionospheric Physics, Chapter 3, p. 94, Academic Press, New York, 1969.
14. N.M. Brice, Bulk Motion of the Magnetosphere, J. Geophys. Res. 72, 5193 (1967).
15. C.R. Chappell, K.K. Harris, and G.W. Sharp, The Morphology of the Bulge Region of the Plasmasphere, J. Geophys. Res. 75, 3848 (1970).